Electronic Structure and Photoelectron Spectroscopy of d^8 Rhodium Indenyl Complexes

Tracey M. Frankcom,† Jennifer C. Green,*,† Atilla Nagy,† Ashok K. Kakkar,‡ and Todd B. Marder*,‡

Inorganic Chemistry Laboratory, South Parks Road, Oxford OX1 3QR, U.K., and Department of Chemistry, University of Waterloo, Waterloo, Ontario N2L 3G1, Canada

Received May 4, 1993®

The parent indenyl compounds (η-C_9H_7)RhL_2 (**1a-c**), trimethylindenyl complexes (η-1,2,3-$Me_3C_9H_4$)RhL_2 (**2a-c**), and permethylindenyl complexes (η-C_9Me_7)RhL_2 (**3a-c**) (**a**, L = η-C_2H_4; **b**, L_2 = η^4-1,5-C_8H_{12}; **c**, L = CO) have been prepared and examined by photoelectron spectroscopy (PES). Extended Hückel molecular orbital calculations were also carried out on (η-C_9H_7)RhL_2 (L = η-C_2H_4, CO). The electron donating ability of the three indenyl ligands, based on the ionization energies of the nonbonding rhodium centered orbitals, is in the order (η-C_9Me_7) > (η-1,2,3-$Me_3C_9H_4$) > (η-C_9H_7). The (η-C_9H_7) (ligand is a stronger donor than (η-C_5H_5). Somewhat lower values of ν_{CO} in the IR spectra and significantly smaller measured barriers to ethylene rotation in the indenyl complexes *vs* their cyclopentadienyl analogues can be traced to weaker Rh–L π-back-bonding, mainly d_{xz}, which is also the acceptor orbital for indenyl π_4. The major factor determining the relative amounts of back-donation is therefore the splitting of the indenyl π_5 and π_4, the two highest lying filled π-orbitals of the indenyl anion, *vs* the degenerate e_1 set of η-C_5H_5 which lies between π_4 and π_5 in energy. A rationale for increased S_N1 substitution rates and catalytic activity of indenyl *vs* cyclopentadienyl complexes is provided.

Introduction

Transition metal indenyl complexes display markedly enhanced reactivity in both stoichiometric[1–18] and catalytic reactions[12,19–24] compared with their cyclopentadienyl analogues. It has been shown,[10,11] for example, that [(η-C_9H_7)$Rh(CO)_2$] (**1c**) reacts with PPh_3 *via* an S_N2 process at a rate which is *ca.* 3.8×10^8 faster than that for [(η-C_5H_5)$Rh(CO)_2$] (**4c**). Permethylation of the indenyl ligand, as in [(η-C_9Me_7)$Rh(CO)_2$] (**3c**), reduces[11,13] the S_N2 rate constant for CO substitution by a factor of *ca* 150 compared with **1c**, yet this is still *ca.* 10^7 faster than that for [(η-C_5Me_5)$Rh(CO)_2$] (**5c**). Interestingly, for [(η-1,2,3-$Me_3C_9H_4$)$Rh(CO)_2$] (**2c**), the rate constant for CO substitution by PPh_3 was only *ca.* 5 times slower[13] than for **1c**. A comparison of the CO stretching frequencies in **1c**-**5c** (Table I)[13] provides some indication of the relative electron density at the metal center in these compounds. Thus it can be seen that methylation of both the indenyl and cyclopentadienyl rings conveys enhanced electron density to the Rh, as expected. On the basis of the data in Table I, it would appear that the C_5H_5 ligand is slightly stronger donor than C_9H_7 and that C_5Me_5 is a stronger donor than C_9Me_7. Electron density at Rh[11,13] is certainly one of several factors influencing the relative rates of ligand substitution in these compounds when methyl groups are added to the ring systems; steric arguments are also important, as are the relative energies of the LUMO's of the various compounds. It is evident, however, for the S_N2 processes, that the relative ease of an η^5–η^3–η^5 coordinative isomerization process in the indenyl compounds must account for the observed "indenyl effect".[10,11]

Rate enhancements of S_N1 type processes have also been observed[3–6] for indenyl *vs* cyclopentadienyl complexes, presumably indicative of weaker metal–ligand bonding in the indenyl species. The rationale for this is not yet understood. Studies[7,25,26] of the barriers to ethylene rotation in the indenyl compounds **1a**, **2a**, and **3a** indicated much smaller activation energies, ranging from 10.3 to

† Inorganic Chemistry Laboratory.
‡ University of Waterloo.
® Abstract published in *Advance ACS Abstracts*, August 15, 1993.

(1) Basolo, F. *Polyhedron* **1990**, *9*, 1503.
(2) O'Connor, J. M.; Casey, C. P. *Chem. Rev.* **1987**, *87*, 307.
(3) White, C.; Mawby, R. J.; Hart-Davis, A. J. *Inorg. Chim. Acta* **1970**, *4*, 441.
(4) White, C.; Mawby, R. J. *Inorg. Chim. Acta* **1970**, *4*, 261.
(5) Turaki, N. N.; Higgins, J. M.; Lebioda, L. *Inorg. Chem.* **1988**, *27*, 424.
(6) Jones, D. J.; Mawby, R. J. *Inorg. Chim. Acta* **1972**, *6*, 157.
(7) Estiagh-Hosseini, M.; Nixon, J. F. *J. Less Common Met.* **1978**, *61*, 107.
(8) Caddy, P.; Green, M.; O'Brien, E.; Smart, L. E.; Woodward, P. *Angew. Chem., Int. Ed. Engl.* **1977**, *16*, 648.
(9) Caddy, P.; Green, M.; O'Brien, E.; Smart, L. E.; Woodward, P. *J. Chem. Soc., Dalton Trans.* **1980**, 962.
(10) Rerek, M. E.; Ji, L. N.; Basolo, F. *J. Chem. Soc., Chem. Commun.* **1983**, 1208.
(11) Rerek, M. E.; Basolo, F. *J. Am. Chem. Soc.* **1984**, *106*, 5908.
(12) Marder, T. B.; Roe, D. C.; Milstein, D. *Organometallics* **1988**, *7*, 1451.
(13) Kakkar, A. K.; Taylor, N. J.; Marder, T. B.; Shen, J. K.; Hallinan, N.; Basolo, F. *Inorg. Chim. Acta* **1992**, *198–200*, 219.
(14) Kakkar, A. K.; Taylor, N. J.; Marder, T. B. *Organometallics* **1989**, *8*, 1765.
(15) Bang, H.; Lynch, T. J.; Basolo, F. *Organometallics* **1992**, *11*, 40.
(16) Ji, L. N.; Rerek, M. E.; Basolo, F. *Organometallics* **1984**, *3*, 740.
(17) Merola, J. S.; Kacmarcik, R. T.; Van Engen, D. *J. Am. Chem. Soc.* **1986**, *108*, 329.
(18) Hart-Davis, A. J.; Mawby, R. *J. Chem. Soc. A* **1969**, 2403.
(19) Caddy, P.; Green, M.; E., S. L.; White, N. *J. Chem. Soc., Chem. Commun.* **1978**, 839.
(20) Borrini, A.; Diversi, P.; Ingrosso, G.; Lucherini, A.; Serra, G. *J. Mol. Catal.* **1985**, *30*, 181.
(21) Ceccon, A.; Gambaro, A.; Santi, S.; Venzo, A. *J. Mol. Catal.* **1991**, *69*, L1.
(22) Bonneman, H. *Angew. Chem. Int., Ed. Engl.* **1985**, *24*, 248.
(23) *Aspects of Homogenous Catalysis*; Bonneman, H., Brijoux, W., Eds.; D. Reidel: Dordrecht, The Netherlands, 1984; Vol. 5, p 75.
(24) Cioni, P.; Diversi, P.; Ingrosso, G.; Lucherini, A.; Ronca, P. *J. Mol. Catal.* **1987**, *40*, 337.
(25) Mlekuz, M.; Bougeard, P.; Sayer, B. G.; McGlinchey, M. J.; Rodger, C. A.; Churchill, M. R.; Ziller, J. W.; Kang, S.-K.; Albright, T. A. *Organometallics* **1986**, *5*, 1656.
(26) Kakkar, A. K.; Taylor, N. J.; Calabrese, J. C.; Nugent, W. A.; Roe, D. C.; Connaway, E. A.; Marder, T. B. *J. Chem. Soc., Chem. Commun.* **1989**, 990.

0276-7333/93/2312-3688$04.00/0

Chart I

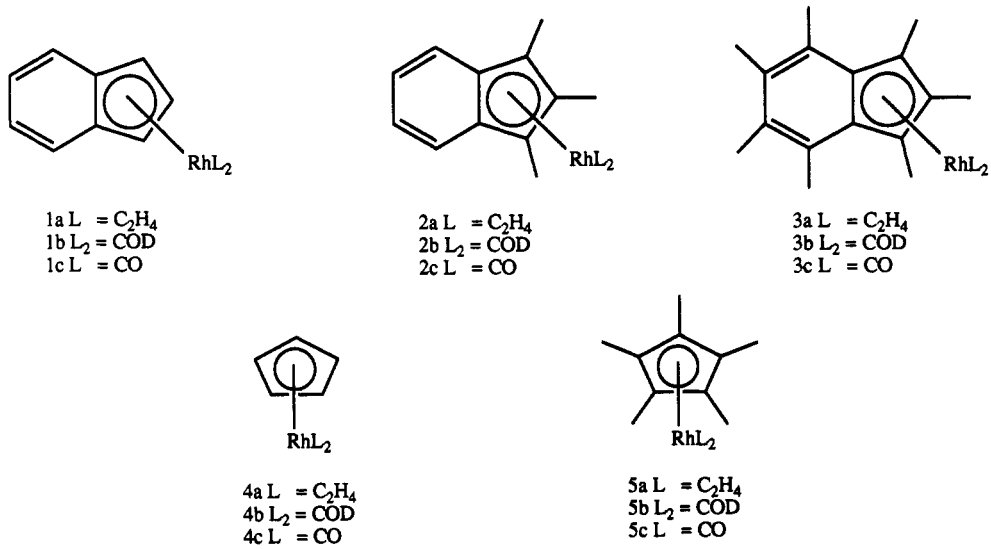

1a L = C_2H_4
1b L_2 = COD
1c L = CO

2a L = C_2H_4
2b L_2 = COD
2c L = CO

3a L = C_2H_4
3b L_2 = COD
3c L = CO

4a L = C_2H_4
4b L_2 = COD
4c L = CO

5a L = C_2H_4
5b L_2 = COD
5c L = CO

Table I. CO Stretching Frequencies for Rhodium Indenyl and Cyclopentadienyl Carbonyl Complexes

compd	ν_{CO}	compd	ν_{CO}
1c	2046, 1991	**4c**	2047, 1984
2c	2035, 1978	**5c**	2024, 1962
3c	2028, 1969		

11.1 ± 0.5 kcal mol^{-1}, for these complexes compared with $\Delta G^{\ddagger}$ values of 15.7 ± 0.2 and 17.1 ± 0.2 kcal mol^{-1} reported[27,28] for C_5H_5 and C_5Me_5 analogues **4a** and **5a**, respectively. This is consistent with the idea of weaker Rh–ethylene π-bonding in, *e.g.*, **1a** *vs* **4a** and the lower thermal stability observed for **1a**. However, it must be appreciated that the rotation barriers are a measure of the differential degree of π-back-bonding between the two rotamers of a given complex and are not necessarily a reflection of the relative strength of the metal–alkene bond in different complexes.

A more detailed knowledge of the electronic structure of the indenyl complexes is required in order to understand the behavior of such systems. As part of our ongoing studies[12–14,26,29–35] of indenyl complexes, we report herein the results of a combined photoelectron spectroscopic and extended Hückel molecular orbital analysis of the electronic structure of a series of rhodium compounds of the form [(η-C_9H_7)RhL_2] (**1a–1c**), [(η-1,2,3-$Me_3C_9H_4$)RhL_2] (**2a–2c**), and [(η-C_9Me_7)RhL_2] (**3a-3c**) [L = η-C_2H_4, L_2 = COD (COD = η^4-1,5-C_8H_{12}), L = CO], shown in Chart I.

Experimental Section

Syntheses. General Procedures. All reactions were performed under a dry nitrogen atmosphere using standard Schlenk and glovebox techniques. Hexane, THF, and diethyl ether were distilled from sodium benzophenone under nitrogen. Heptamethylindene was prepared according to a literature procedure[35] which is a modification of that originally reported.[36] The 1,2,3-trimethylindene was prepared via a modification of previously published procedures,[37–39] and details are provided below. Tigloyl chloride was prepared according to a published procedure.[35] Compounds **1a**,[7–9,29] **1b**,[7–9,25] **1c**,[7–9,26] **2c**,[13] and **3c**[11,13] were prepared by literature routes. The ^1H and $^{13}C\{^1H\}$ NMR spectra were recorded on a Bruker AC200, AM250, or AM400 spectrometer.

Trimethylindene (1,2,3-$Me_3C_9H_5$). A mixture of tigloyl chloride (11.7 g, 0.1 mmol) and anhydrous $AlCl_3$ (48 g, 360 mmol) in benzene (100 mL) was refluxed for 16 h and, upon cooling, poured into a mixture of ice (200 g) and concentrated HCl (100 mL). The organic layer was washed with a saturated solution of sodium chloride (50 mL, ×2) and a saturated solution of $NaHCO_3$ (50 mL, ×2) and then dried over anhydrous $MgSO_4$. After the removal of the solvent, 2,3-dimethylindan-1-one (14 g, 87.5% yield) was obtained as an orange oily liquid. MeLi (20 mL, 1.4 M, 0.028 mol) was added dropwise at 0 °C to a solution of this ketone (4 g, 0.025 mol) in diethyl ether (50 mL). The mixture was refluxed for 16 h and then quenched with a saturated solution of ammonium chloride (15 mL). After removal of the solvent from the organic layer under reduced pressure, a light yellow liquid was obtained. it was mixed with iodine (50 mg), and the mixture was heated to 100 °C for 2 h. The dark brown product was extracted into ether (100 mL), and washed sequentially with water (25 mL, ×2) and 10% aqueous $Na_2S_2O_4$ (25 mL, ×2), and then dried over anhydrous sodium sulfate. The orange liquid obtained was purified by chromatography on a silica column using hexane–ethyl acetate (8:1) and subsequently by distillation under reduced pressure, yielding 1,2,3-trimethylindene (3.2 g, 82% yield) as a very light yellow liquid. ^1H NMR (C_6D_6, 200 MHz): δ 1.14 (d, J_{H-H} = 7 Hz, 3H, CH_3 at C_3), 1.78 (s, 3H, CH_3 at C_1), 1.91 (s, 3H, CH_3 at C_2), 3.00 (q, 1H, H at C_3), 7.2 (m, 4H, H_{4-7}). $^{13}C\{^1H\}$ NMR (C_6D_6, 50 MHz): δ 10.1, 11.8, 15.8 (s, CH_3), 47.1 (s, C_3), 118.3, 122.3 (s, $C_{1,2}$), 126.7, 127.1, 129.4, 131.3 (s, C_{4-7}).

[(η^5-1,2,3-$Me_3C_9H_4$)$Rh(\eta$-$C_2H_4)_2$] (2a).[26] Trimethylindene (158 mg, 1 mmol) was deprotonated with *n*-BuLi (1.6 M, 0.6 mL, 1 mmol) in diethyl ether (10 mL) for 24 h. The resulting suspension was added to an ether (15 mL) solution of [$(C_2H_4)_2$-$Rh(\mu$-Cl)$]_2$ (194 mg, 0.5 mmol) and stirred for 24 h. The ether was removed under reduced pressure and the resulting dark solid extracted with hexane. After purification on alumina, **2a** (183

(27) Cramer, R.; Mrowca, J. J. *Inorg. Chim. Acta* **1971**, *5*, 528.
(28) Arthurs, M. A.; Nelson, M. A. *J. Coord. Chem.* **1983**, *13*, 29.
(29) Marder, T. B.; Calabrese, J. C.; Roe, D. C.; Tulip, T. H. *Organometallics* **1987**, *6*, 2012.
(30) Kakkar, A. K.; Jones, S. F.; Taylor, N. J.; Collins, S.; Marder, T. B. *J. Chem. Soc., Chem. Commun.* **1989**, 1454.
(31) Marder, T. B.; Williams, I. D. *J. Chem. Soc., Chem. Commun.* **1987**, 1478.
(32) Carl, R. J.; Hughes, R. P.; Reingold, A. L.; Marder, T. B.; Taylor, N. J. *Organometallics* **1988**, *7*, 1613.
(33) Westcott, S. A.; Kakkar, A. K.; Stringer, G.; Taylor, N. J.; Marder, T. B. *J. Organomet. Chem.* **1990**, *394*, 777.
(34) Crossley, N. S.; Green, J. C.; Nagy, A.; Stringer, G. *J. Chem. Soc., Dalton Trans.* **1989**, 2139.
(35) O'Hare; Green, J. C.; Marder, T.; Collins, S.; Stringer, G.; Kakkar, A. K.; Kaltsotannis, N.; Kuhn, A.; Lewis, R.; Mehnart, C.; Scott, P.; Kurmoo, M.; Pugh, S. *Organometallics* **1992**, *11*, 48.
(36) Miyamoto, T. K.; Tsutsui, M.; Chen, L. B. *Chem. Lett.* **1981**, 729.
(37) Miller, W. G.; Pittman, C. U. *J. Org. Chem.* **1974**, *39*, 1955.
(38) Pittman, C. U.; Miller, W. G. *J. Am. Chem. Soc.* **1973**, *95*, 2947.
(39) Plattner, P. A.; Fürst, A.; Jerasek, K. *Helv. Chim. Acta* **1947**, *30*, 1320.

Table II

Structures and Parameters[45] Used in the Extended Hückel Calculations

atom	orbital	H_{ii}	exponent
Rh	5s	−8.09	2.135
	5p	−4.57	2.099
	4d	−12.5	4.290 (0.5870), 1.970 (0.5685)
C	2s	−21.4	1.625
	2p	−11.4	1.625
O	2s	−32.3	2.275
	2p	−14.8	2.275
H	1s	−13.6	1.300

Bond Distances (Å) and Angles (deg) Assumed in the Extended Hückel Calculations

	$Rh(\eta\text{-}C_9H_7)(CO)_2$	$Rh(\eta\text{-}C_9H_7)(C_2H_4)_2$
Rh—ring perpendicular	1.945	1.902
slip	0.25	0.101
ring C—C	1.427	1.435
C—H	1.09	1.09
Rh—C carbonyl	1.807	
C—O carbonyl	1.132	
C—Rh—C angle	91.7	
Rh—C=C perpendicular		2.031
C—C ethene		1.377
C—H ethene		1.07
ethene centroid—Rh—ethene centroid		96.3

mg, 58% yield) was obtained as a yellow solid. ^{1}H NMR (C_6D_6, 250 MHz): δ 1.62 (s, 6H, CH_3), 1.91 (s, 8H, C_2H_4), 2.00 (d, J_{Rh-H} = 1.5 Hz, 3H, CH_3), 7.14 (m, 4H, H_{4-7}). $^{13}C\{^1H\}$ NMR (C_6D_6, 62.9 MHz): δ 7.7 (s, CH_3), 10.9 (s, CH_3), 48.0 (d, J_{Rh-C} = 13 Hz, C_2H_4), 86.5 (s, $C_{1,3}$), 106.9 (s, C_2), 110.8 (s, $C_{3a,7a}$), 117.2, 123.0 (s, C_{4-7}).

[(η^5-1,2,3-$Me_3C_9H_4$)Rh(η^4-1,5-COD)] (2b). Trimethylindene (158 mg, 1 mmol) was deprotonated with *n*-BuLi (1.6 M, 0.6 mL, 1 mmol) in diethyl ether (10 mL) for 24 h. The resulting suspension was added to an ether (15 mL) solution of [(1,5-COD)Rh(μ-Cl)]$_2$ (220 mg, 0.44 mmol), and the mixture was stirred for 24 h. The ether was removed under reduced pressure and the resulting dark solid extracted with hexane. After purification on alumina, **2b** (200 mg, 54% yield) was obtained as a yellow solid. ^{1}H NMR (C_6D_6, 200 MHz): δ 1.75 (s, 6H, CH_3), 1.88 (m, 8H, COD), 2.11 (d, J_{Rh-H} = 1.6 Hz, 3H, CH_3), 3.47 (br s, 4H, COD, 7.16 (m, 4H, H_{4-7}). $^{13}C\{^1H\}$ NMR (C_6D_6, 100.6 MHz): δ 8.4, 11.0 (s, CH_3), 31.8 (s, COD), 71.2 (d, J_{Rh-C} = 14 Hz, COD), 85.2 (s, $C_{1,3}$), 107. 4 (s, C_2), 112.0 (s, $C_{3a,7a}$), 117.3, 122.1 (s, C_{4-7}).

[(η^5-C_9Me_7)Rh(η-C_2H_4)$_2$] (3a). Heptamethylindene (107 mg, 0.5 mmol) was deprotonated with *n*-BuLi (1.6 M, 0.32 mL, 0.5 mmol) in THF (15 mL) for 24 h. The resulting suspension was added to a THF solution of [$(C_2H_4)_2$Rh(μ-Cl)]$_2$ (97 mg, 0.25 mmol) and stirred for 48 h. THF was removed under reduced pressure and the resulting dark solid extracted with hexane. After purification on alumina, **3a** (260 mg, 70% yield) was obtained as a yellow solid. ^{1}H NMR (C_6D_6, 250 MHz): δ 1.77 (s, 8H, C_2H_4), 2.00 (s, 6H, CH_3), 2.14 (s, 3H, CH_3). 2.22 (s, 6H, CH_3) 2.41 (s, 6H, CH_3). $^{13}C\{^1H\}$ NMR (C_6D_6, 62.9 MHz): δ 11.3, 12.1, 16.7, 17.0 (s, CH_3), 47.4 (d, J_{Rh-C} = 13 Hz, C_2H_4), 86.9 (s, $C_{1,3}$), 106.8 (d, J_{Rh-C} = 6 Hz, C_2), 109.1 (s, $C_{3a,7a}$), 124.0, 130.2 (s, C_{4-7}).

[(η^5-C_9Me_7)Rh(η^4-1,5-COD)] (3b).[30] Heptamethylindene (107 mg, 0.5 mmol) was deprotonated with *n*-BuLi (1.6 M, 0.32 mL, 0.5 mmol) in THF (15 ml) for 24 h. The resulting suspension was added to a THF solution of [(1,5-COD)Rh(μ-Cl)]$_2$ (110 mg, 0.22 mmol) and stirred for 48 h. THF was removed under reduced pressure and the resulting dark solid extracted with hexane. After purification on alumina, **3b** (180 mg, 67% yield) was obtained as a yellow solid. ^{1}H NMR (C_6D_6, 200 MHz): δ 1.86 (m, 8H, COD), 1.96 (s, 3H, CH_3), 2.06 (s, 3H, CH_3), 2.13 (s, 6H, CH_3), 2.41 (s, 6H, CH_3), 3.60 (br s, 4H, COD). $^{13}C\{^1H\}$ NMR (C_6D_6, 50.3 MHz): δ 11.4, 12.9, 16.7, 17.1 (s, CH_3), 32.3 (s, COD), 70.7 (d, J_{Rh-C} = 14 Hz, COD), 85.6 (s, $C_{1,3}$), 107.2 (s, C_2), 110.0 (s, $C_{3a,7a}$), 123.6, 129.4 (s, C_{4-7}).

Photoelectron Spectroscopy. Photoelectron spectra were recorded on a PES Laboratories 0078 spectrometer interfaced with a Research Machines 380Z microprocessor. The instrumental resolution gave a fwhm of 20 meV for the first band of N_2 at the commencement of each run, though in some cases it deteriorated to 30 meV during the course of a measurement. The spectra were calibrated using He, N_2, and Xe. Band areas were determined for **1a, 1b, and 3c** by curve fitting the spectra, and the relative He II/He I band area ratio ($R_{2/1}$ value) was normalized to that of the first band in each spectrum.

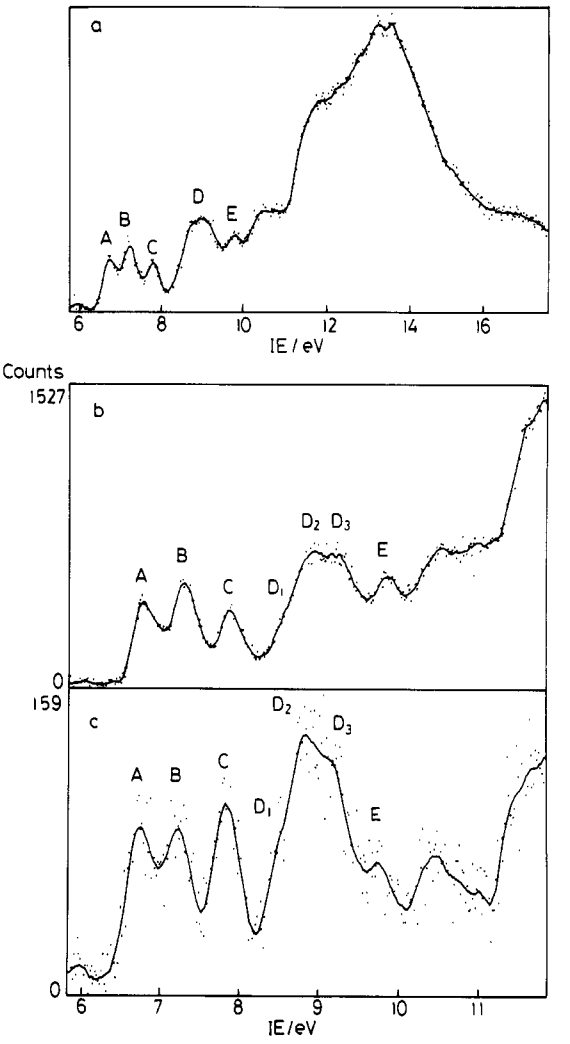

Figure 1. He I (a and b) and He II (c) spectra of $Rh(\eta\text{-}C_9Me_7)(CO)_2$, **3c**.

Theoretical Calculations. Extended Hückel molecular orbital calculations were performed on **1a** and **1c**. The structural information and parameters used are listed in Table II. The structures and axis system assumed are shown in Figure 5.

Results

Thermal stability proved a problem in obtaining the spectra of some compounds. Stability increased with methylation of the ring, in spite of increased sublimation temperatures, and also in the order CO < C_2H_4 < COD. Of the carbonyl compounds only the heptamethylindenyl compound yielded a satisfactory spectrum.

The spectra are given in Figures 1–3; the points represent the experimental data and the line a least squares fit to these points. For **3c** the full range He I spectrum is shown together with He I and He II scans of the low ionization energy (IE) region. For the other compounds, though data were collected over the full range, only the He I and He II scans of the low IE region are given. Vertical IE are tabulated (Table II) together with $R_{2/1}$ values (He II/He

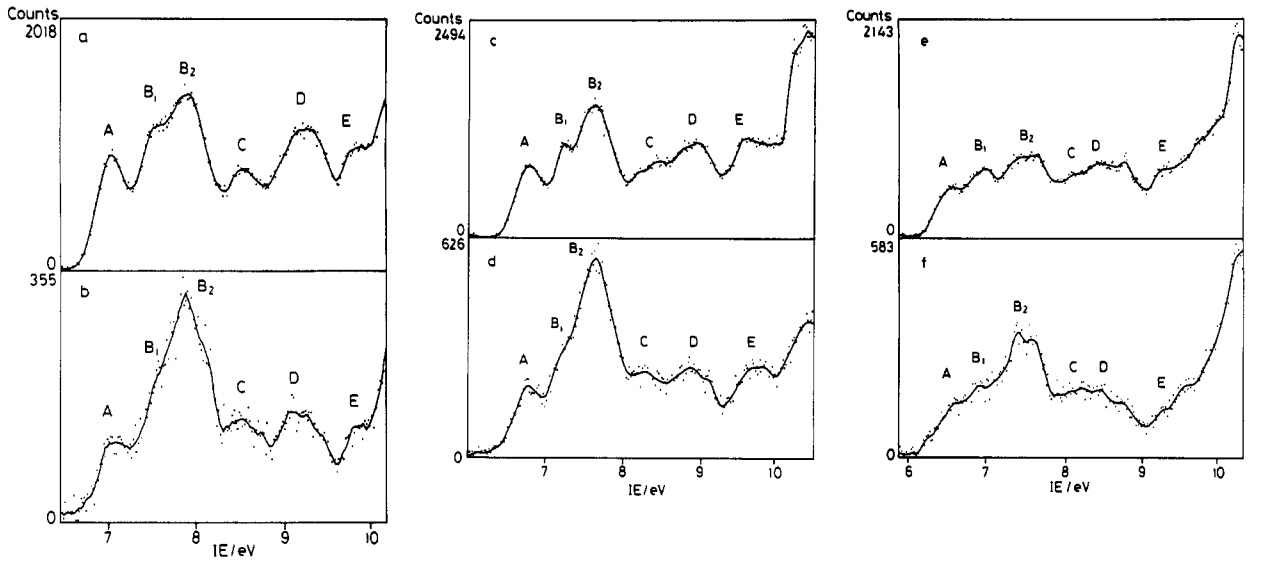

Figure 2. He I and He II spectra of Rh(η-C_9H_7)(C_2H_4)$_2$, **1a** (a, He I; b, He II), Rh(η-$C_9H_4Me_3$)(C_2H_4)$_2$, **2a** (c, He I; d, He II), and Rh(η-C_9Me_7)(C_2H_4)$_2$, **3a** (e, He I; f, He II).

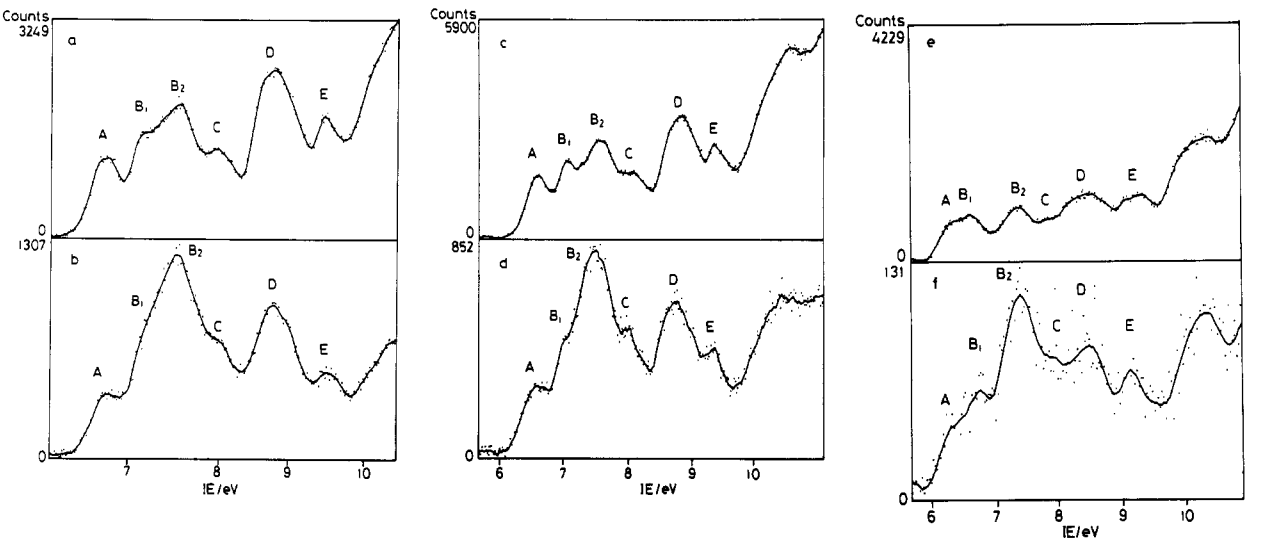

Figure 3. He I and He II spectra of Rh(η-C_9H_7)(COD), **1b** (a, He I; b, He II), Rh(η-$C_9H_4Me_3$)(COD), **2b** (c, He I; d, He II), and Rh(η-C_9Me_7)(COD), **3b** (e, He I; f, He II).

I band intensity ratios) (Table III). Figure 4 gives a graphical representation of the trends found in the vertical IE of the complexes.

Discussion

For the purpose of the description of the electronic structure, we consider the indenyl ligand to have a mirror plane, and for the calculation we assume equal C–C bond lengths. The projection of the Rh atom onto the indenyl plane is slipped away from the η^5 position toward η^3.

Simple MO arguments predict that the RhL_2 unit should straddle the mirror plane of the indenyl fragment, as is found to be the case for **1c**. A single crystal structure determination of **2a** showed the RhL_2 unit to be rotated 21.2° away from this idealized symmetry in the solid state.[26] However, apparent mirror symmetry in solution, as evidenced by NMR, suggests energy differences between the two conformations are small. In general, overall C_s symmetry is assumed. The choice of axes for the molecules is given in Figure 5.

The bonding in indenyl d^8 compounds is expected to resemble that of the analogous cyclopentadienyl compounds which have already been the subject of MO calculations and PES studies.[40–43] The published data will be used to assist with assignment of the spectra under investigation. Figure 6 shows the projection onto the xy plane of the nine indenyl π orbitals, five of which are filled. The three highest lying occupied π MO's, π_5, π_4, and π_3, resemble the degenerate e_1 HOMO of the cyclopentadienyl anion, having one nodal plane cutting through the C_5 ring, and as such, might be expected by symmetry arguments to interact with the d_{xy} and d_{yz} orbitals of the metal fragment. Such overlap will be greater for π_5 than for π_3 since the former is more localized on the C_5 ring and it also lies closer in energy to the metal d orbitals. The cyclopentadienyl e_1 orbitals lie between π_4 and π_5 in energy.

The metal center will have four occupied d orbitals, and we would expect to observe ionizations from all of these in the low energy region of a PE spectrum.[40–42] Ionizations from π_1 and π_2 will lie in the region of the σ bands and will

(40) Dudeney, N.; Kirchner, O. N.; Green, J. C.; Maitlis, P. M. *J. Chem. Soc., Dalton Trans.* **1984**, 1877.
(41) Green, J. C.; Powell, P.; van Tilborg, J. E. *Organometallics* **1984**, *3*, 211.
(42) Lichtenberger, D. L.; Calabro, D. C.; Kellog, G. E. Organometallics **1984**, *3*, 1623.

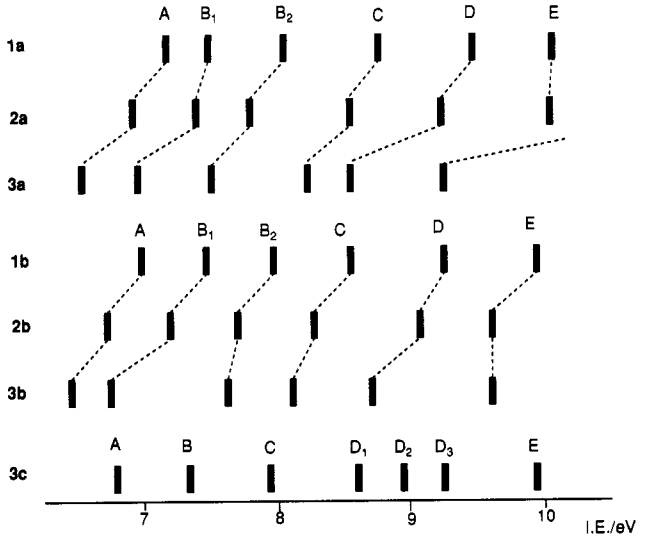

Figure 4. Trends in vertical IE for **1a**, **2a**, **3a**, **1b**, **2b**, **3b**, and **3c**.

Table III. Vertical Ionization Energies (eV) of Rhodium Indenyl Compounds

band	1a	2a	3a
A	7.19	6.90	6.53
B_1	7.73	7.39	6.97
B_2	8.07	7.81	7.53
C	8.77	8.55	8.23
D	9.46	9.23	8.56
E	10.09	10.05	9.26
band	**1b**	**2b**	**3b**
A	6.98	6.72	6.43
B_1	7.46	7.21	6.73
B_2	7.95	7.70	7.61
C	8.57	8.27	8.08
D	9.25	9.08	8.68
E	9.94	9.62	9.60

band	3c
A	6.80
B	7.36
C	7.93
D_1	8.61
D_2	8.96
D_3	9.25
E	9.92

not be identifiable.[34] The band associated with π_3 will also lie close to this region and may be difficult to assign. Ionization bands from π_4 and π_5 should occur in the low energy region of a spectrum.

The simplest spectrum is expected from the carbonyl complexes, as CO itself has no ionization bands below 14 eV. As noted above, it was not possible to obtain a high quality spectrum for **2c**: therefore only the spectrum of **3c** will be discussed. Seven features may be identified with vertical IE below 10 eV, A, B, C, D_1, D_2, D_3, and E. From $R_{2/1}$ values A, C, and D have the most metal character. More detailed assignments can be made after consideration of the MO calculations which delineate the nature of the interactions between indenyl and the Rh$(CO)_2$ fragment.

Calculations on 1c. Extended Hückel MO calculations,[44] including fragment analyses, were performed in order to obtain an approximate MO composition. Figure 7 shows the orbital energy sequence predicted by the calculations for **1c**, and Figure 8 represents the key MO's. In the Rh$(CO)_2$ fragment, the d_{yz} orbital is destabilized by interaction with the CO 5σ orbitals. The $d_{x^2-y^2}$ and d_{z^2} orbitals are rehybridized to give a nonbonding d_{x^2} orbital, and the d_{xy}, d_{xz}, and $d_{z^2-y^2}$ orbitals are all involved in back-bonding to the 2π orbitals of the CO ligands. Strong interaction occurs between the indenyl π_4 orbital and the d_{xz} orbital of the metal to form bonding and antibonding orbitals (38 and 33). The indenyl π_5 orbital interacts less strongly with the metal d_{yz} antibonding orbital to form MO 34 which has significant metal character. (Metal d_{yz} is also used for σ donation by the CO ligands.) MO 35 is almost solely metal based, the major contribution being from a d_{x^2}-like orbital on the Rh$(CO)_2$ fragment, and is nonbonding in character. MO 36 results from the interaction of d_{xy} with π_5 and is predominantly metal in character, as is MO 37 which has large coefficients from d_{z^2} and $d_{x^2-y^2}$ giving a $d_{z^2-y^2}$ type orbital with significant CO back-bonding character. The π_3 orbital does not appear to contribute significantly to any of these MO's and fragment analysis shows it to contribute to mainly lower lying MOs 39 and 41. The metal characters of the various MO's are listed in Table IV.

PE Spectral Assignment of 3c. The $R_{2/1}$ values of **3c** indicate that band A, C, and D are from orbitals largely localized on the metal. Band B has a lower $R_{2/1}$ value, suggesting that it should be assigned to MO 34, the bonding combination of π_5 and the d_{yz} orbital, which is largely ligand based, having a calculated metal character of 12%. Band E has the lowest $R_{2/1}$ value and lies close to the σ bands at 9.92 eV. This band is therefore assigned to MO 39, which is the π_3 orbital of the indenyl ligand. The $R_{2/1}$ ratio is at its largest for band C and is therefore assigned to MO 35 which is calculated to have metal character of 85%. The ionization of 6.80 eV (band A) is assigned to the HOMO, MO 33, which is calculated to have 32% metal character and is the antibonding combination of π_4 and the d_{xz} orbital. A similar assignment has been made for the first band of the PE spectra of **4c** and **5c**.[40,42]

Assignment of bands D_1, D_2, and D_3 to the remaining MO is difficult, since separate areas are difficult to estimate for overlapping bands and therefore individual $R_{2/1}$ values would be unreliable. However, on inspection it appears that band D_3 falls in intensity relative to bands D_1 and D_2 on passing from He I to He II radiation. On the basis of this observation, band D_3 is assigned to MO 38, the bonding combination of π_4 and d_{xz}, which has a lower metal character than either MO 36 or MO 37, to which bands D_1 and D_2 are therefore assigned.

It should be noted that the ordering of the bands, in this case, corresponds with the MO ordering. The latter is, to a certain extent, a function of the parameterization of the calculation. In related studies of cyclopentadienylrhodium compounds, a similar correspondence has been found.

Calculations on 1a. Figure 5 shows the structure adopted for the study of **1a**. Figure 9 shows the orbital energy sequence predicted by the calculations, and Figure 10 represents some key MO's. For the rhodium bis(ethylene) fragment, d_{yz} is destabilized by donation from the ethylene π-electrons. The orbitals d_{xy} and d_{xz} are involved in back-donation to the ethylene π^* orbitals and

(43) Dodds, A. S. Part II Thesis, Oxford University, 1986.
(44) Hoffman, R. *J. Chem. Phys.* **1963**, *39*, 1397.
(45) Summerville, R. H.; Hoffmann, R. *J. Am. Chem. Soc.* **1976**, *98*, 7240.

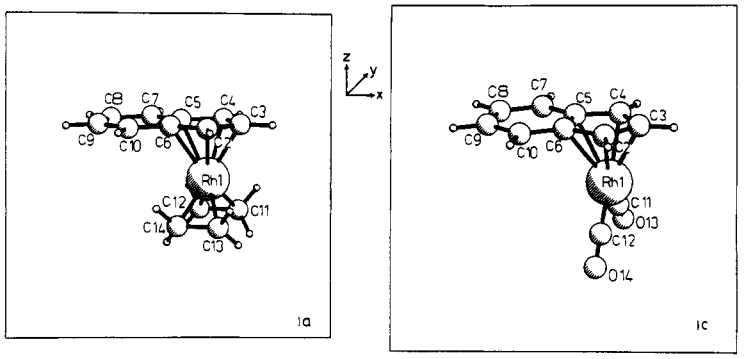

Figure 5. Structures and coordinate systems assumed for **1a** and **1c**.

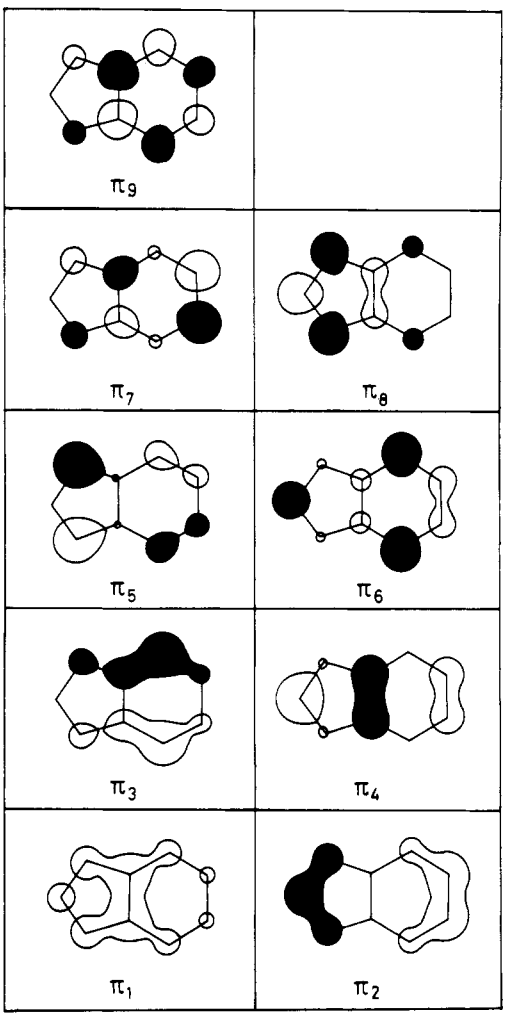

Figure 6. Projection onto the *xy* plane of the nine indenyl π orbitals.

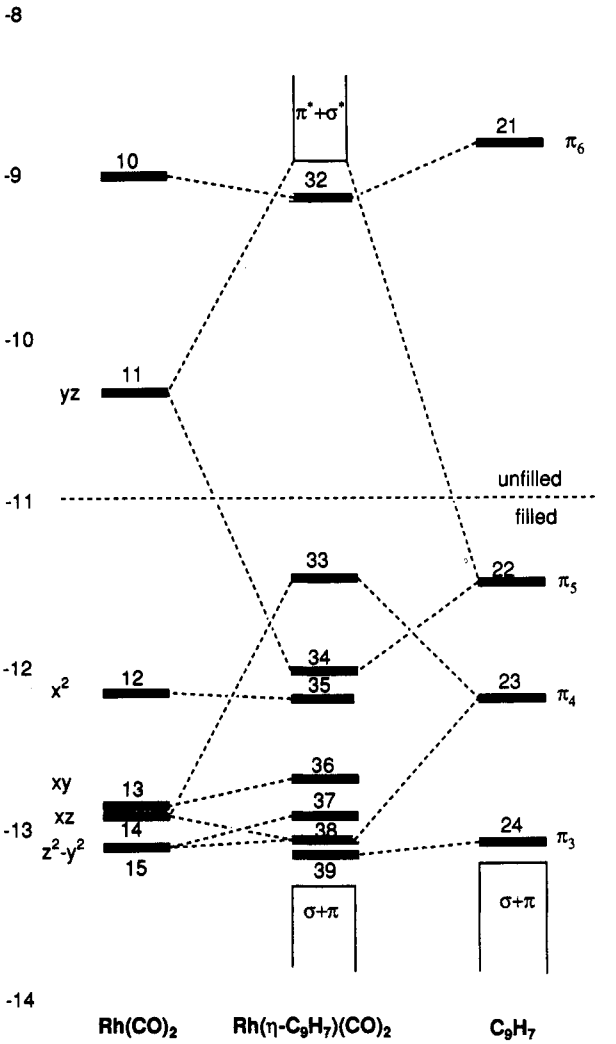

Figure 7. MO diagram for **1c**.

d_{z^2} and $d_{x^2-y^2}$ are more or less nonbonding; they do not rehybridize as is found for the $Rh(CO)_2$ fragment.

The HOMO 39 is the antibonding combination of π_4 of the indenyl ligand with the d_{xz} orbital of the metal, MO 44 being the bonding combination. MO's 40 and 42 are strongly metal based, resulting from the d_{z^2} and $d_{x^2-y^2}$ orbitals; some rehybridization seems to occur on interaction with the indenyl ring. The indenyl π_5 orbital interacts with the antibonding d_{yz} orbital to form MO 41 which has a high degree of ligand character. MO 43 is mainly d_{xy} in character, retaining the small degree of backbonding character mentioned above. The indenyl π_3 ligand is found to be the chief contributor to the lower lying MO 45. The ethylene π orbitals correlate with MO 48 and MO 49.

PE Spectral Assignment of the Bis(ethylene)-rhodium Indenyl Compounds. The band structure is most distinctive for **1a** and **2a**, that of **3a** being less well defined. The assignment is therefore based on the former pair of compounds.

Six features may be identified below 10.5 eV (Figure 2), and these are labeled A, B_1, B_2, C, D, and E. From $R_{2/1}$ values bands B (B_1 + B_2) and C have the highest metal character. The general effect of methylating the indenyl ligand is to shift all bands observed in the PE spectrum to lower IE (Figure 4), with bands A and B_1 showing the greatest relative shifts (the shoulder B_1 becomes more distinct on moving from C_9H_7 to 1,2,3-$Me_3C_9H_4$), suggesting that these bands correspond to ionizations more localized on the indenyl ligands. Though the B bands, B_1

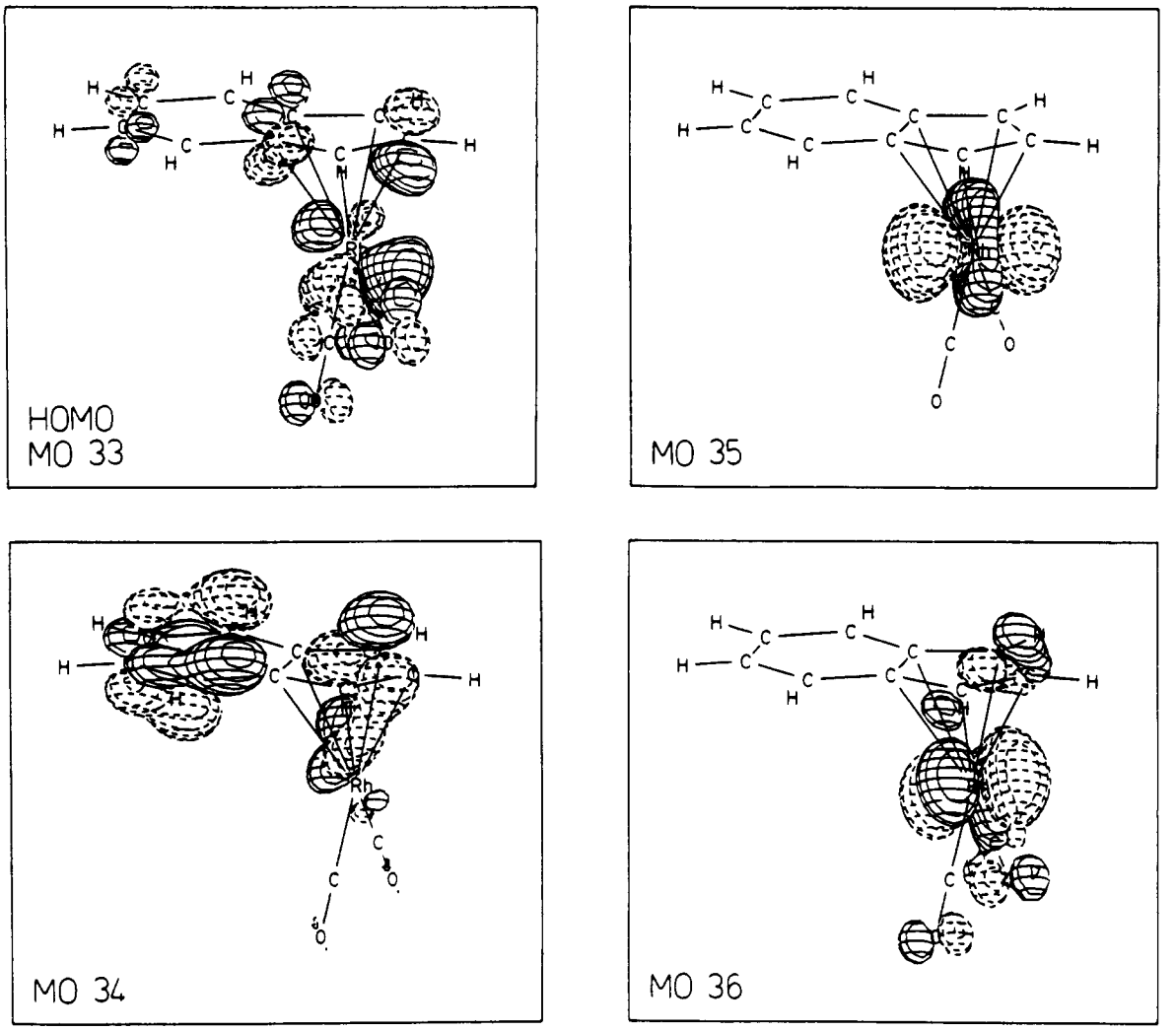

Figure 8. Selected MO for **1c**.

Table IV. Relative Band Intensities, Percentage Metal Character, and Band Assignments

	band character[a]	rel intens He I	rel intens He II	$R_{2/1}$	assgnt	MO[a]	% metal
1a	A	1.00	1.00	1.00	d_{xz}/π_4	39	35
	B_1	2.92	4.25	1.45	d_{yz}/π_5	41	13
	B_2				$d_{x^2-y^2} + d_{z^2}$	40 + 42	85 + 83
	C	0.94	1.19	1.27	d_{xy}	43	63
	D	1.79	1.95	1.09	d_{xz}/π_4	44	18
	E	1.78	1.52	0.85	$C_2H_4\ \pi$	48	9
1b	A	1.00	1.00	1.00	d_{xz}/π_4		
	B_1	3.29	5.36	1.63	d_{yz}/π_5		
	B_2				$d_{x^2-y^2} + d_{z^2}$		
	C	0.75	1.13	1.51	d_{xy}		
	D	3.57	2.99	0.84	d_{xz}/π_4+		
	E	1.49	0.89	0.59	COD π		
3c	A	1.00	1.00	1.00	d_{xz}/π_4	33	32
	B	1.11	0.77	0.69	d_{yz}/π_5	34	12
	C	0.73	1.23	1.68	d_{x^2}	35	85
	D_1	4.52	3.53	0.78	d_{xy}	36	62
	D_2				$d_{x^2-z^2}$	37	47
	D_3				d_{xz}/π_4	38	29
	E	1.41	0.43	0.30	π_3	39	2

[a] Based on extended Hückel calculations on **1a** and **1c**.

and B_2, overlapped too much to have their intensities assessed independently, the band profile strongly suggests that B_1 decreases in intensity relative to B_2 in the He II spectrum compared with the He I spectrum. They are therefore assigned to the highest MO's with significant ligand character, i.e. MO 39 and MO 41. The $R_{2/1}$ values show that bands B and C have the most metal character, while intensity data suggest that band B_2 actually corresponds to ionization from two metal orbitals. Therefore band B_2 is assigned to the nonbonding, metal based orbitals MO 40 and MO 42, which have calculated metal characters of 85% and 83%, respectively. Band C is assigned to the remaining orbital of high metal character MO 43 (63%), and band D, to the bonding combination of π_4 and d_{xz}, which has low metal character (18%). The first and second bands of the carbonyl and ethene compounds thus have similar assignments.

Though the calculations indicate that the next band should arise from the indenyl π_3 orbital, it shows little energy shift between **1a** and **2a** (0.04 eV), suggesting that a more likely origin is the ethylene π orbitals MO 48 and MO 49. However, on further methylation to **3a**, a substantial shift is observed, suggesting that in the case of **3a**, band E should be assigned to an indenyl π_3 ionization.

The assignment we prefer for the first four bands differs from the orbital ordering of the top four filled levels in the calculation. The experimental reasons for assigning band B_1 to an orbital with significant indenyl content is clear and the assignment corresponds to that found for **3c**. As the orbital ordering in the extended Hückel calculation is to a certain extent a function of the parameterization, there is no reason to expect that it will faithfully reproduce the ionization energy sequence. Rather, we see the role of the calculation as giving an indication of the orbital

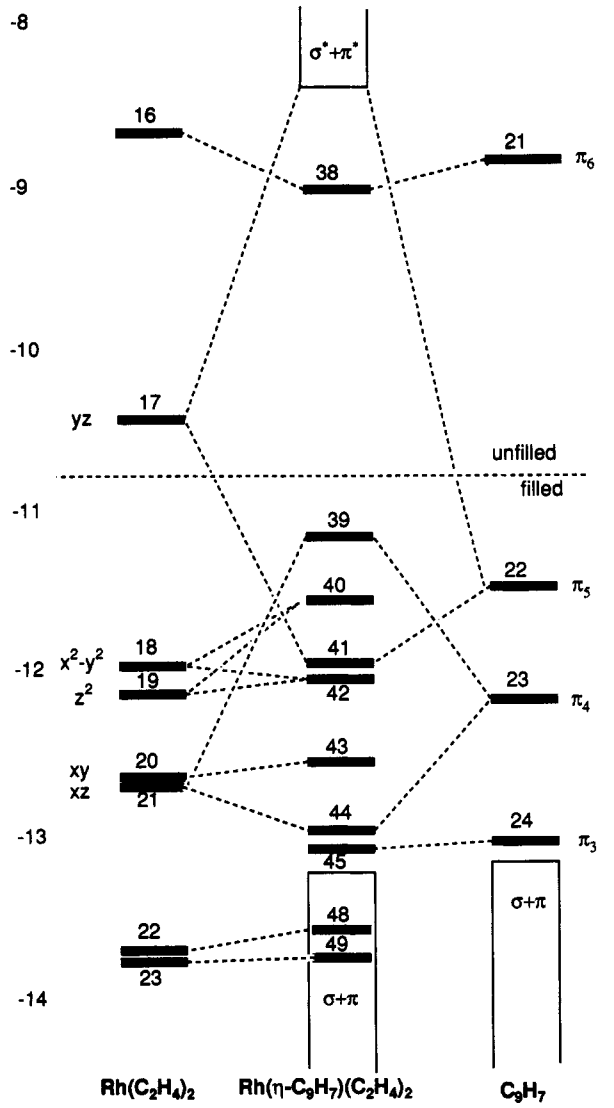

Figure 9. MO diagram for **1a**.

structure clearer than can be obtained by symmetry and electronegativity arguments on their own.

Spectral Assignment of the Cyclooctadienerhodium Indenyl Compounds. The PE spectra of the cyclooctadiene compounds may be assigned by comparison with those of the bis(ethylene) compounds whose spectra they resemble closely. Again the heptamethylindenyl compound, **3b** (Figures 3e,f) has a less clearly defined spectrum than the other two, **3a** and **3c** (Figures 2e,f and Figure 1, respectively).

Six features are notable in the low energy region of the PE spectrum, these being at slightly lower IE than the corresponding bands of the analogous ethylene compounds. The same labeling scheme is adopted, although for the cyclooctadiene compounds band C lies much closer to band B, almost becoming a second shoulder. Bands B and C are again found to have the largest $R_{2/1}$ values, indicating the highest metal character. A contrast with the ethylene spectra is that band D, rather than band E, shows the smallest shift in energy on changing from C_9H_7 to 1,2,3-$Me_3C_9H_4$. However, on further methylation to C_9Me_7 E shows the smaller change. The relative shifts by all other bands on methylation are similar to one another. However, band B_1 does not become more distinct as it did in the spectra of the ethylene compounds. This suggests that there may be a greater degree of mixing of fragment orbitals within the MO of the cyclooctadiene compounds.

From $R_{2/1}$ values, bands B and C are again found to have the most metal character. Though independent $R_{2/1}$ values cannot be determined for band B_1 and B_2, it is apparent, by eye, that the shoulder (B_1) does not show the same increase in intensity as is seen for the main band (B_2) on passing from He I to He II radiation. On this basis, bands A, B_1, B_2, and C are given the same assignment as they were in the ethylene case. Bands D and E both have low $R_{2/1}$ values, indicating little metal character, although band E has notably the lower value, which would appear to suggest the band E is attributable to ionizations from a cyclooctadiene orbital. However, a larger shift is observed in the energy of this band on moving from C_9H_7 to 1,2,3-$Me_3C_9H_4$ (0.32 eV for E compared to 0.17 eV for D), whereas on further methylation to C_9Me_7 the larger shift is in band D (0.40 eV for D compared with 0.02 eV for E). The most obvious way to account for these irregular trends is to postulate a greater degree of orbital mixing in the cyclooctadiene compounds so that the approximation of localized ligand ionizations fails. This situation was also found for the closely related cobalt and rhodium cyclopentadienyl diene complexes.[41] Further, intensity data suggest that band D may arise from ionizations from two molecular orbitals. Thus bands D and E are assigned to MO's which represent mixtures of a d_{xz}/π_4 bonding MO, a high lying cyclooctadiene orbital, and the indenyl π_3 orbital.

Comparison with Rhodium Cyclopentadienyl Compounds. Having assigned the PE spectra, we are now in a position to address the questions of reactivity and ligand dynamics raised in the Introduction. In Table IV we summarize the first vertical IE for the indenyl compounds studied here and related rhodium cyclopentadienyl and pentamethylcyclopentadienyl complexes. The best measure we have of relative charge on the metal center is the IE of the nonbonding metal orbitals, MO 40 and 42 of the diene complexes giving rise to band B_2 and MO 35 of the carbonyl compounds giving rise to band C. A previous study of core IE shifts in **4c** and **5c**[42] showed that the nonbonding orbital had shifts on methylation very similar to that of the Rh $3d_{5/2}$ ionization. The IE values of these nonbonding bands are given in Table V together with those of analogous cyclopentadienyl- and (pentamethylcyclopentadienyl)rhodium compounds. Errors in these IE's should be taken as ±0.1 eV.

Methylation of either indenyl or cyclopentadienyl lowers the IE. The first IE is affected rather more than a nonbonded IE because the first ionization arises from an orbital with ring character. Comparison between the indenyl and cyclopentadienyl $Rh(C_2H_4)_2$ complexes puts indenyl as a stronger donor to the metal than cyclopentadienyl. This was also found to be the case for the ferrocene and ruthenocene indenyl analogues.[34] The relative positions of the methylated derivatives is less clear, the order depending on the particular series examined. Probably the most important factor accounting for the increased donor strength of the indenyl ligand is the high energy of π_5 compared with the equivalent cyclopentadienyl e_1 orbital.

The relative donor strengths of C_5H_5 and C_9H_7, as indicated by the IE, are somewhat surprising in light of the lower CO stretching frequencies found for **4c** (Table I) compared with **1c**. One of the orbitals back-donating

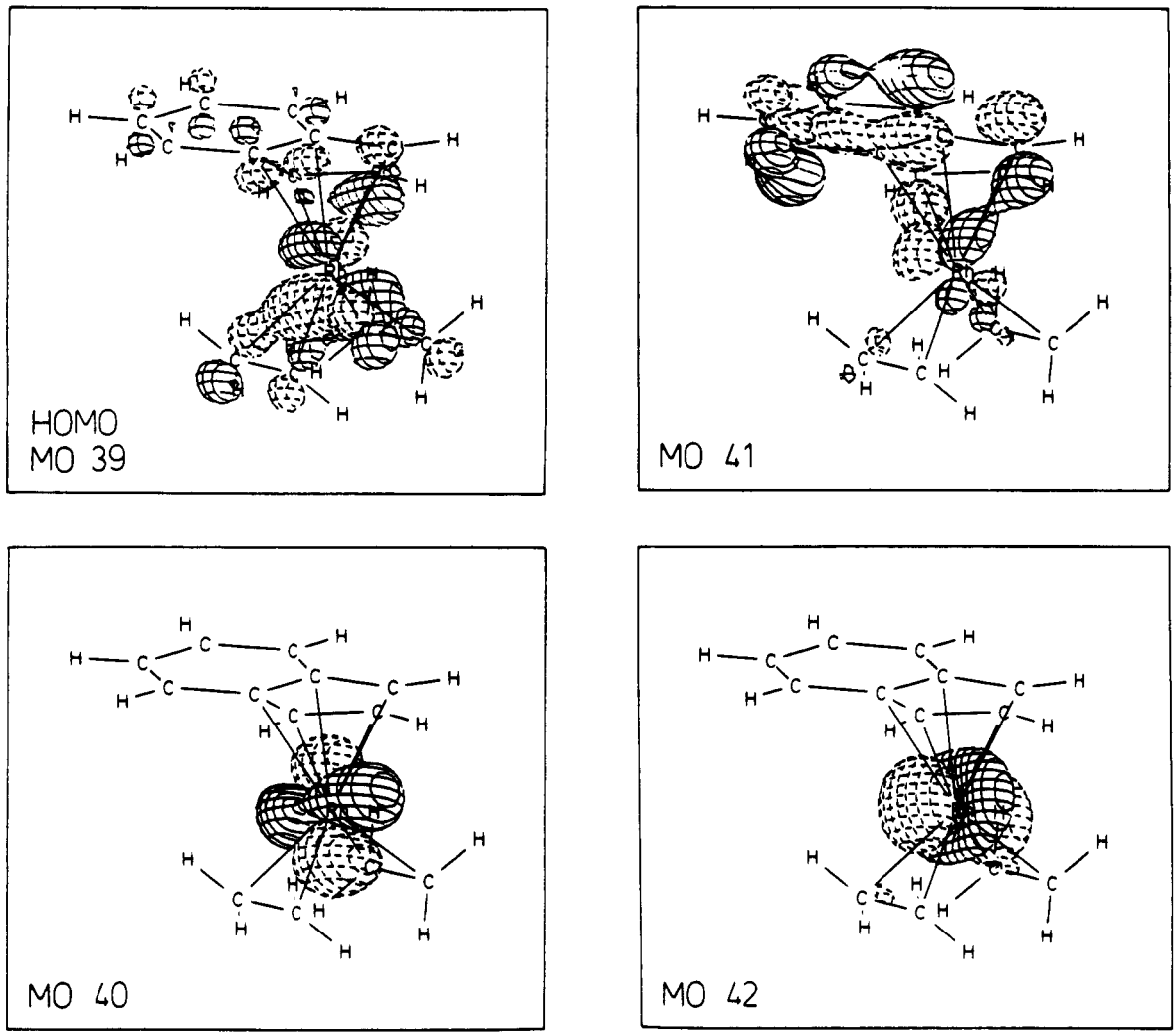

Figure 10. Selected MO for 1a.

Table V. First IE of Rhodium Indenyl and Cyclopentadienyl Complexes[40-43]

	1	2	3	4	5
a	7.19	6.90	6.53	7.33	6.92
b	6.98	6.72	6.43	7.07	6.36
c			6.80	7.64	6.80

Table VI. IE of Nonbonding Orbitals in Rhodium Indenyl and Cyclopentadienyl Complexes[40-43]

	1	2	3	4	5
a	8.07	7.81	7.53	8.27	8.05
b	7.95	7.70	7.61	8.00	7.67
c			7.93	8.65	8.12

to the carbonyls is d_{xz}, which is also the acceptor orbital for donation from π_4. The donation to CO is thus, in part, directly linked to π_4. As noted above, π_4 lies lower in energy (that is it has a more negative orbital energy) than the e_1 C_5H_5 levels, thus making donation from the ring to the metal d_{xz} orbital, and hence back-donation to the carbonyl groups, less effective in the indenyl compound than in the cyclopentadienyl case.

Similar considerations should apply to the bis(ethylene) compounds. In these the d_{xy} and d_{xz} orbitals are responsible for back-donation to the ethylene ligands. The d_{xy} orbital has 63% Rh character (and is metal ring nonbonding) consistent with it having δ symmetry with respect to the ring. Band C, arising from this orbital is perturbed less than, for example, band A upon ring alkylation. Thus, d_{xy} will be less sensitive to changes in the ring system and as such will have little influence on the *relative* degree of π-back-bonding to ethylene in the cyclopentadienyl *vs* indenyl complexes. However, indenyl π_4 again shares the d_{xz} orbital for bonding (Figure 9) so back-bonding to the ethylene in the preferred rotamer is expected to be less effective for **1a** than for **4a**. This is a possible reason for the lower rotational barriers in the indenyl compounds.[7,25,26] Likewise, band B_2 arising from $d_{x^2-y^2}$ and d_{z^2}, the M–ring σ interaction is virtually pure metal in character. The d_{z^2} orbital is of appropriate symmetry for π-back-bonding to ethylene when the ethylene ligands are rotated through 90° with respect to their preferred rotational orientation. This band (B_2) lies at higher energy than the nonbonding levels for **4a**, suggesting back-bonding to ethylene somewhat stronger *in the rotated conformer* for **1a** *vs* that for **4a**. The differential π-back-bonding between the two rotamers (presumably related directly to the barrier height) will be influenced to some extent by the d_{z^2} orbital energies in the cyclopentadienyl *vs* indenyl complexes. Therefore, both destabilization of the ground state as well as some stabilization of the transition state can contribute to the significantly smaller barriers observed for the indenyl compounds.

Conclusions

Photoelectron spectroscopic studies indicate that indenyl ligands are somewhat stronger electron donors to d^8

ML_2 fragments than are their cyclopentadienyl counterparts. This conclusion is based on the relative ionization energies of the metal based, i.e. nonbonding, orbitals of the cyclopentadienyl and indenyl compounds. Substitution of indenyl ring hydrogens by methyl groups enhances further the electron donor ability of indenyl rings in a fashion similar to that observed in cyclopentadienyl compounds. This increased electron richness at Rh should enhance oxidative addition chemistry.

Whereas dramatically enhanced S_N2 substitution rates[1-11,13-19,31] for indenyl *vs* cyclopentadienyl compounds can be attributed to enhanced propensity for ring slippage (see for example ref 33 and references therein) in indenyl systems, the enhanced rates observed for S_N1 substitutions[3-6] of ethylene or CO ligands in indenyl compounds would, at first glance, seen inconsistent with the increased electron density at Rh which would be expected to lead to stronger metal–ligand back-bonding. However, ethylene rotation barriers are lower and CO stretching frequencies are higher for indenyl than for cyclopentadienyl compounds. These factors indicate *less efficient* M–CO and M–ethylene back-bonding in the indenyl compounds even though the electron density at Rh is higher. This apparent dichotomy can be explained by a detailed examination of the specific orbitals involved in π-back-bonding. The differences can be traced, at least to a large extent, to the splitting of the π_4 and π_5 levels of the indenyl ligand. These orbitals are related to the degenerate e_1 set of the π orbitals of the cyclopentadienyl ligand which fall between indenyl π_4 and π_5 in energy. The lower energy of π_4 *vs* cyclopentadienyl e_1 results in less effective π-back-bonding to CO and ethylene in the indenyl compounds. This is entirely consistent with (1) higher ν_{CO} values, (2) lower ethylene rotation barriers, and (3) weaker M–L bonding, leading to more facile dissociation and the enhancement of S_N1 substitution rates, as observed for the indenyl complexes. A combination of greater electron density at Rh and more facile ligand dissociation also contributes to the enhanced catalytic activity of the indenyl complexes.

Acknowledgment. We thank the Soros Foundation (A.N.) the SERC (J.C.G.), the Royal Society, the Natural Sciences and Engineering Research Council of Canada, and Imperial Oil Ltd. (T.B.M.) for financial support.

OM9302913